

1 **Understanding the role of surface oxygen-containing functional groups**
2 **on carbon-supported cobalt catalysts for oxygen evolution reaction**

3 Thi Ha My Pham,^{a,b} Youngdon Ko,^{a,b} Manhui Wei,^{a,b,c} Kangning Zhao,^d Liping Zhong,^{a,b,*} Andreas Züttel^{a,b}

4

5 ^aLaboratory of Materials for Renewable Energy (LMER), Institute of Chemical Sciences and Engineering
6 (ISIC), Basic Science Faculty (SB), Ecole Polytechnique Fédérale de Lausanne (EPFL) Valais/Wallis,
7 Energypolis, Rue de l'Industrie 17, CH-1951 Sion, Switzerland

8 ^bEMPA Materials & Technology, CH-8600 Dübendorf, Switzerland

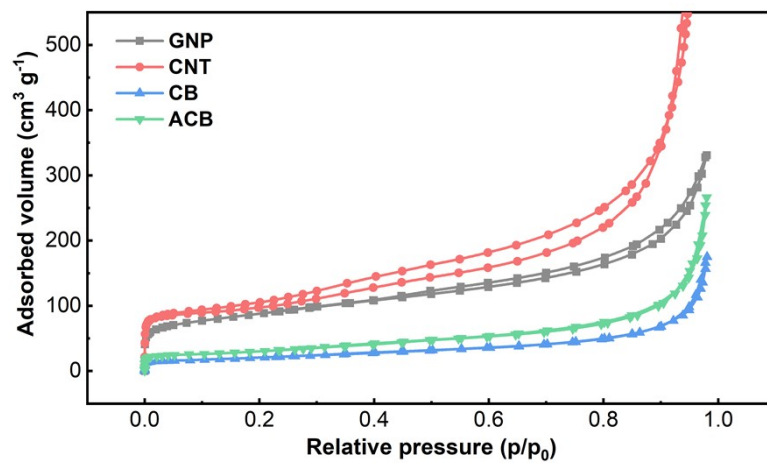
9 ^cSchool of Mechanical Engineering, Beijing Institute of Technology, Beijing 100081, P. R. China

10 ^dLaboratory of Advanced Separations, Ecole Polytechnique Federale de Lausanne, Sion, Switzerland

11

12

13 E-mail: liping.zhong@epfl.ch



15

16 Figure S1 N₂ adsorption-desorption as a function of relative pressure, acquired by N₂-adsorption measurements on
17 the four fresh supports.

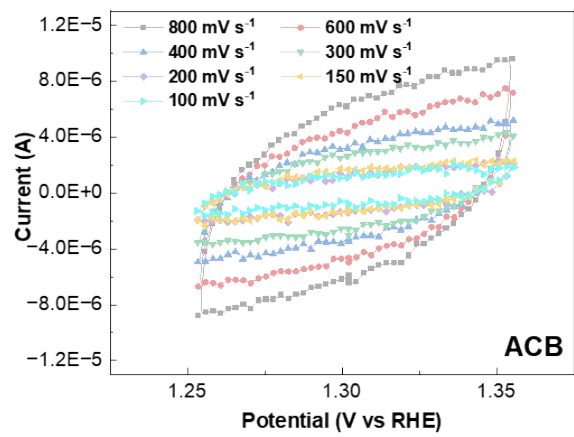
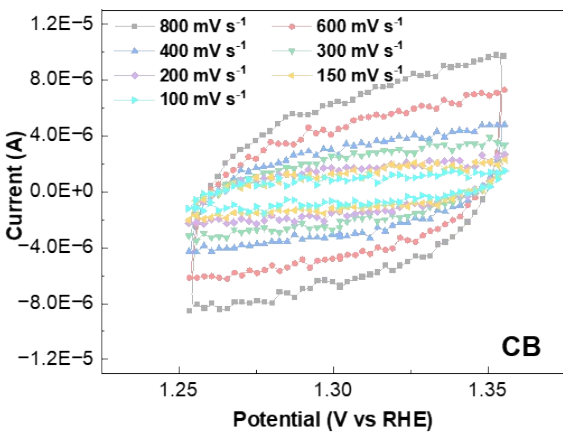
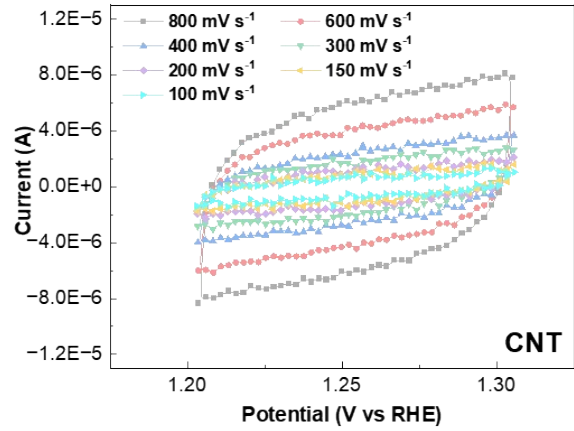
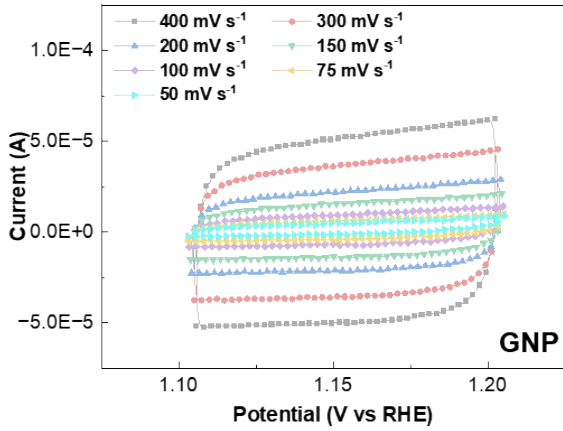
18

19 Table S1 Summary of the BET surface area of the four fresh supports, derived from the N₂ adsorption-desorption
20 measurements using BET method.

Support	BET surface area (m² g⁻¹)
CNT	368
ACB	107
CB	74
GNP	310

21

22



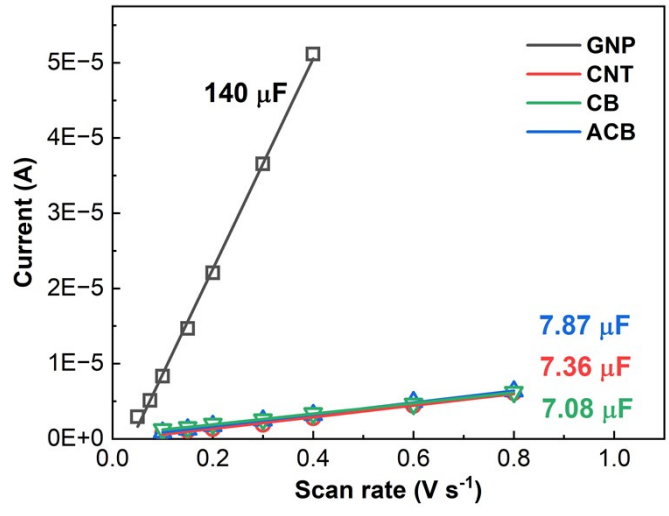
23

24 Figure S2 Double-layer capacitance measurements for different carbon supports. The sub-figures plot the current as
 25 a function different scan rate.

26

27

28

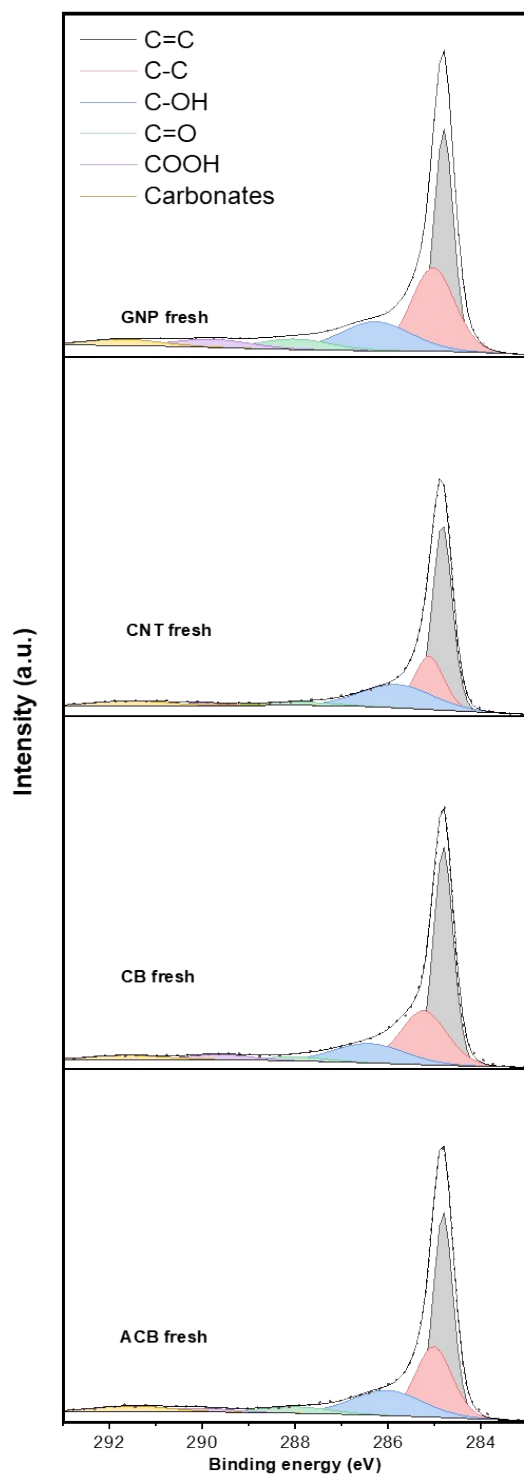


29

30 Figure S3 Linear regression of the measured charging currents as a function of the scan rate. The slope of the line
 31 corresponds to the double-layer capacitance.

32

33



34

35 Figure S4 XPS C 1s spectra of the four supports, and the fitted peaks for carbon (C=C and C-C), surface oxygen
 36 containing groups (COH, COOH and C=O), and surface carbon oxygenates

37

38

39 Table S2 Summary of the surface concentration of oxygen and s-OFGs, measured on the four fresh supports.

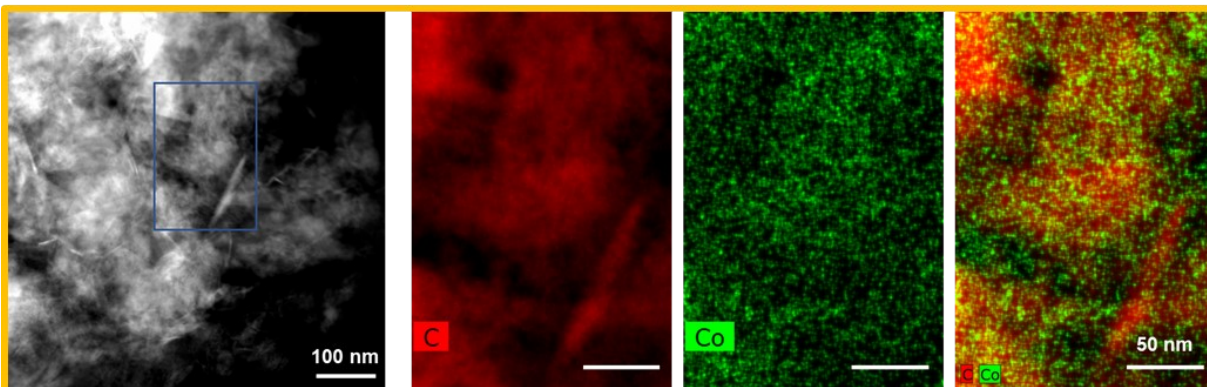
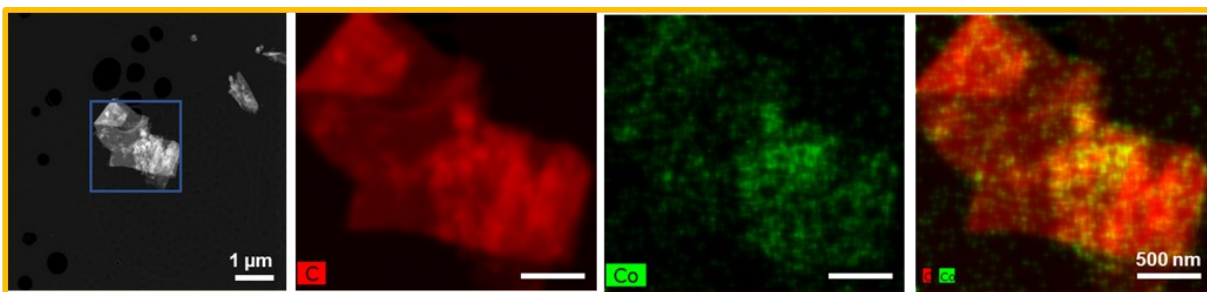
	Oxygen (%)	COH (%)	COOH (%)	C=O (%)
GNP	3.32	1.48	0.32	1.37
CB	3.51	1.32	0.32	1.72
ACB	1.15	0.38	0.21	0.49
CNT	0.65	0.12	0.23	0.31

41 Table S3 Co contents in the synthesized catalysts: GNP-0.5, CNT-0.5, CB-0.5 and ACB-0.5, averaged from 2 sets of
42 measurements

Co concentration (%)	
GNP	0.51 ± 0.01
CNT	0.57 ± 0.23
CB	0.46 ± 0.23
ACB	0.53 ± 0.10

43

44



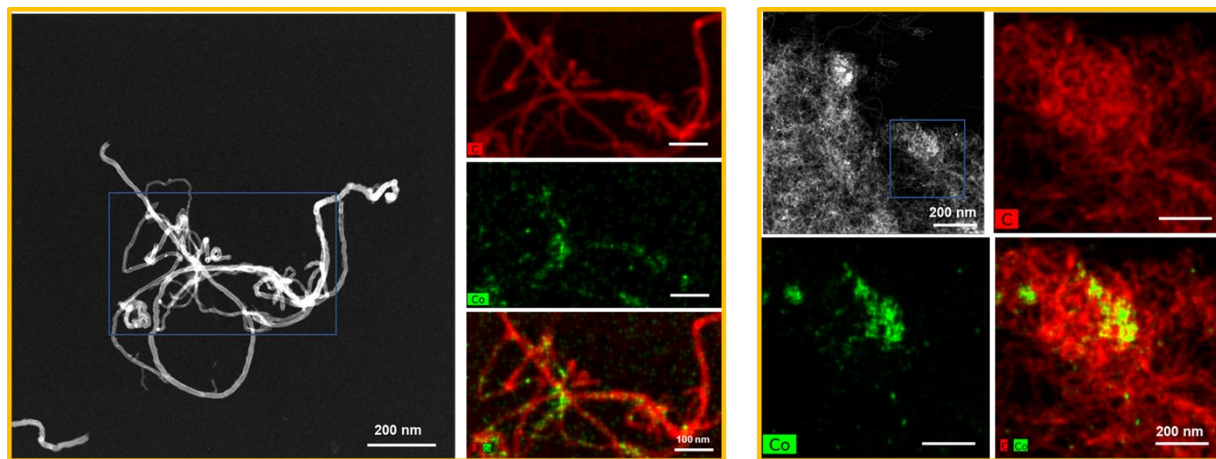
45

46 Figure S5 HAADF-STEM images and the corresponding elemental maps for C and Co, obtained at two different regions

47 on GNP-0.5.

48

49

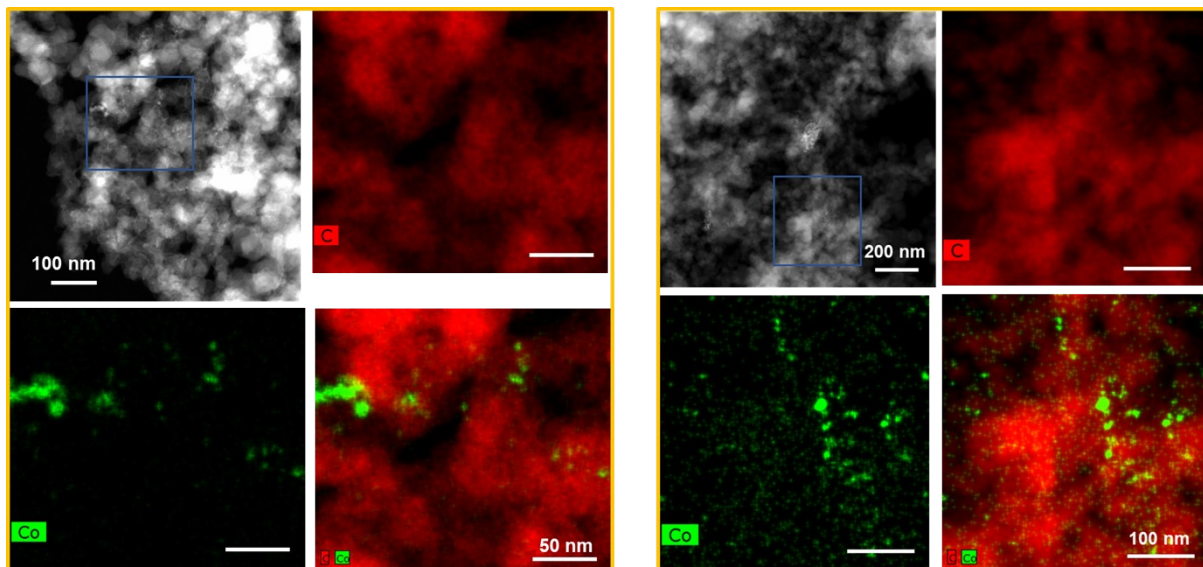


50

51 Figure S6 HAADF-STEM images and the corresponding elemental maps for C and Co, obtained at two different regions
52 on CNT-0.5.

53

54



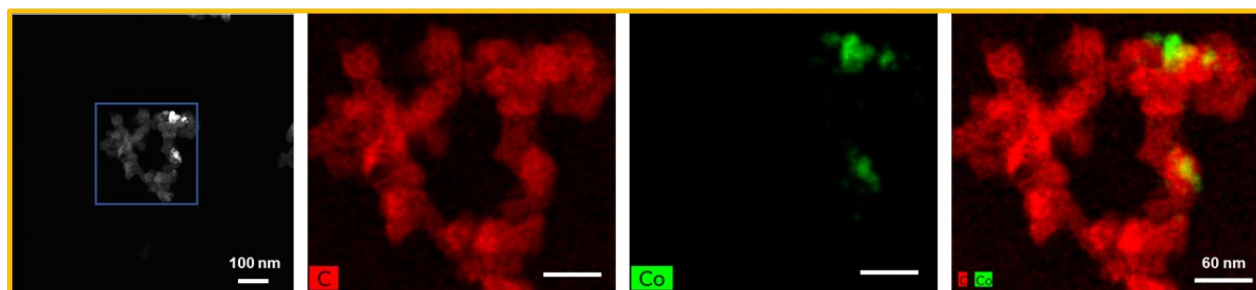
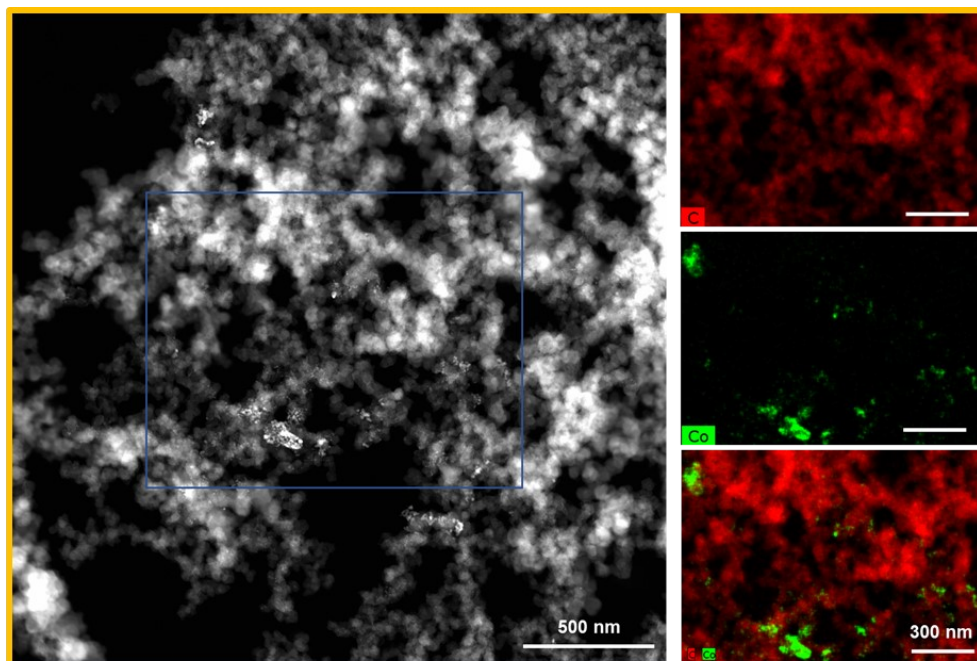
55

56 Figure S7 HAADF-STEM images and the corresponding elemental maps for C and Co, obtained at two different regions

57 on CB-0.5.

58

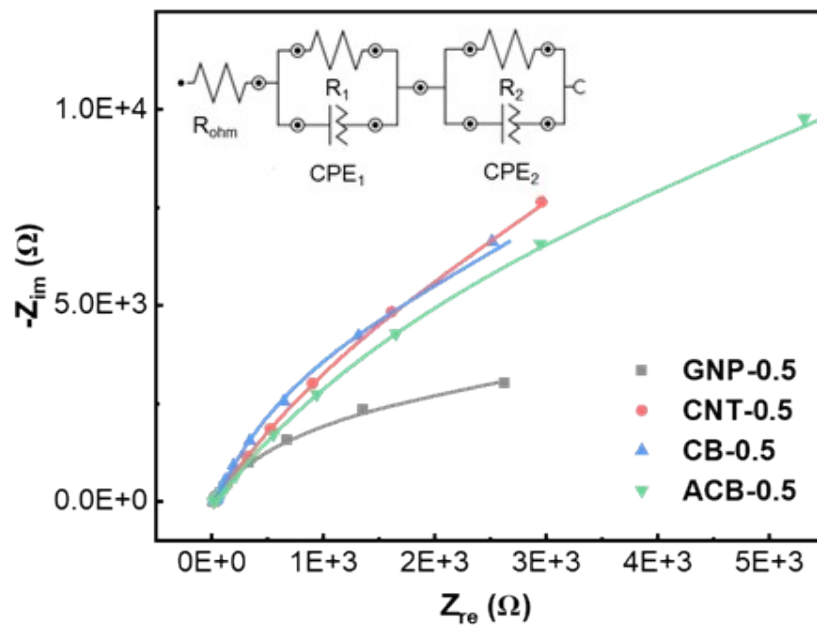
59



60

61 Figure S8 HAADF-STEM images and the corresponding elemental maps for C and Co, obtained at two different regions
62 on ACB-0.5.

63

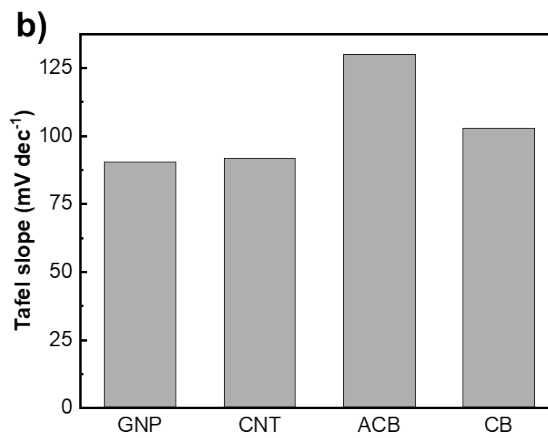
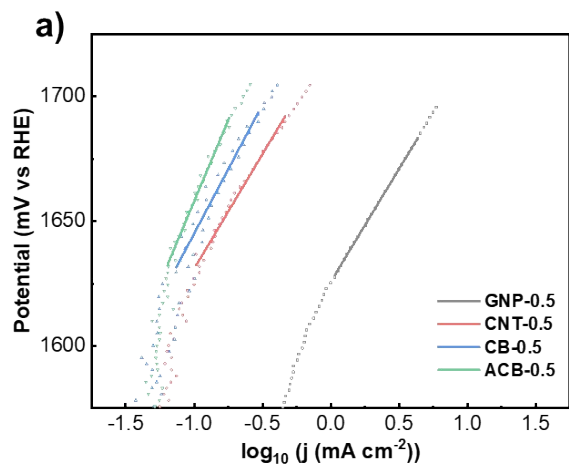


65

66 Figure S9 Nyquist plot and the fitted curve according to the corresponding equivalent circuit. The EIS was acquired

67 at 1.5 V vs RHE, with a perturbation amplitude of ± 10 mV, from 100 kHz to 0.1 Hz.

68



69

70 Figure S10 a) Tafel plots and b) the corresponding Tafel slopes of Co-catalyst supported on four different carbons.

71

72 Table S4 Mass activities of previously reported Co-based catalysts.

References	Samples	Overpotential (V vs RHE)	Mass activity ($A\ g^{-1}$)
A ^[1]	Co SAC	1.65	2209
B ^[2]	BN/CA-NiCoFe-600	1.6	201
C ^[3]	Co _{0.7} Fe _{0.3} CB	1.55	643
D ^[4]	Ir-networks (Ir:Co = 1:55)	1.53	800
E ^[5]	SL-Co(OH) ₂	1.58	153.8
F ^[6]	Au-Co(OH) ₂	1.5	177
G ^[7]	γ -CoOOH nanosheets	1.53	66.6
H ^[8]	YRCO-560	1.48	49.75
I ^[9]	EtOH-CoO	1.7	2900
J ^[10]	ECA-Co _x Ni _{1-x} S ₂	1.57	217

73

74

75

76

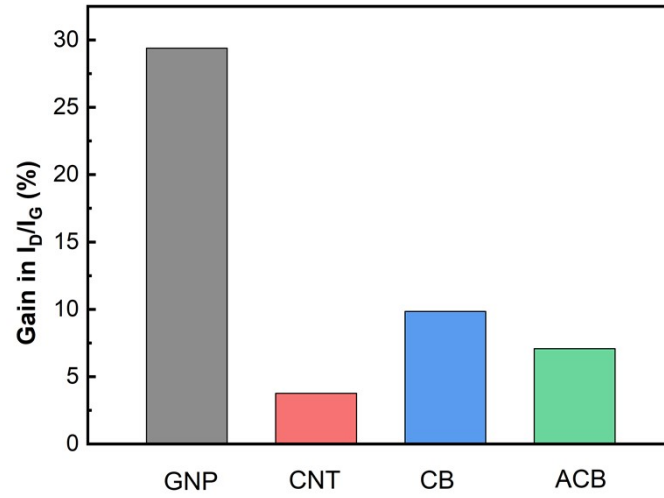
77

78 Table S5 Summary of I_d/I_g ratio of the fresh- and doped- carbon, determined with Raman spectroscopy. The presented
79 value was obtained from at least 10 different regions.

Support	Fresh	With Co doping
GNP	0.11 ± 0.02	0.15 ± 0.06
CNT	0.76 ± 0.11	0.79 ± 0.09
CB	1.11 ± 0.04	1.22 ± 0.04
ACB	1.12 ± 0.03	1.20 ± 0.04

80

81



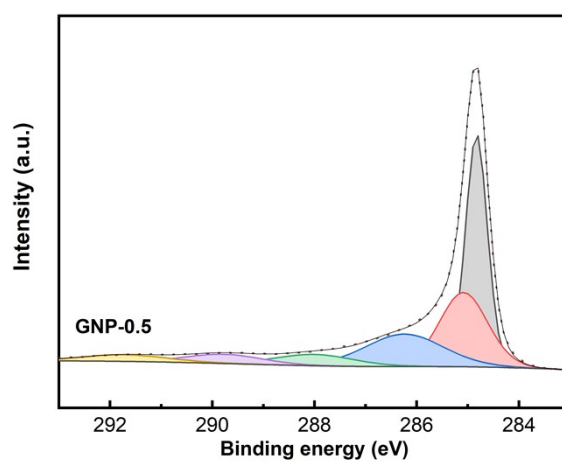
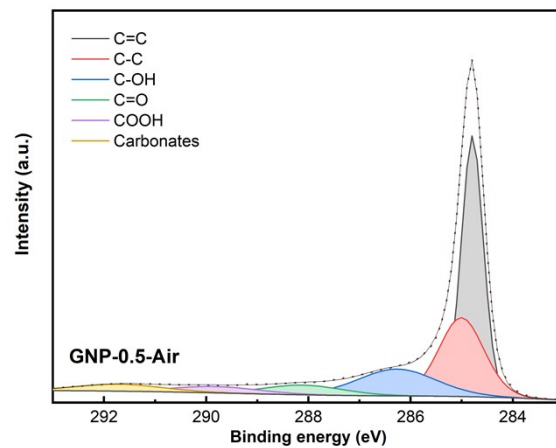
83

84 Figure S11 The gain in I_d/I_g between before and after Co-incorporation. This value is calculated as the quotient

85 between $[I_d/I_{g[\text{Co-doped}]} - I_d/I_{g[\text{fresh support}]}]$ and $[I_d/I_{g[\text{fresh support}]}]$.

86

87



88

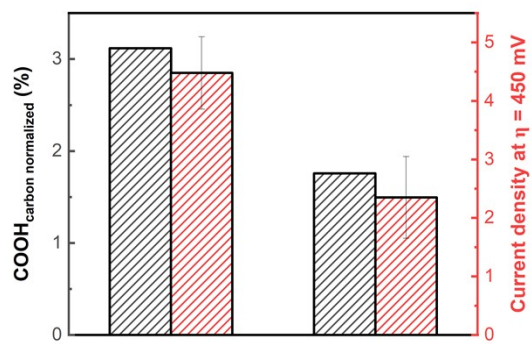
89 Figure S12 XPS C 1s spectra of GNP-0.5-Air and GNP-0.5 and the corresponding deconvoluted peaks.

90

- 91 Table S6 Summary of the s-OFGs surface concentration on the fresh GNP support, GNP-0.5-Air and GNP-0.5. The s-
- 92 OFGs surface concentration is the ratio [area of s-OFGs fitted in O 1s spectra] to [total area of carbon in C 1s spectra].

	GNP support	GNP-0.5-Air	GNP-0.5
Oxygen surface contents (%)	3.21	3.47	4.37
C=O surface concentration (%)	1.37	1.53	1.00
COH surface concentration (%)	1.48	1.49	1.96
COOH surface concentration (%)	0.32	0.27	1.15

93

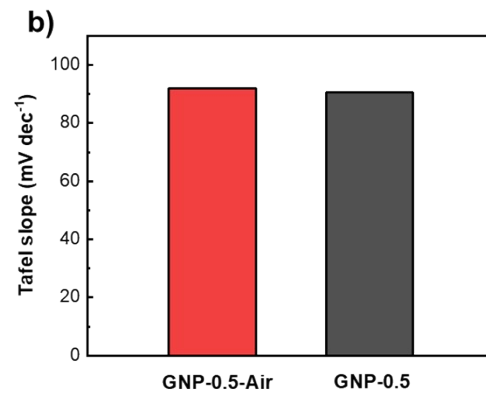
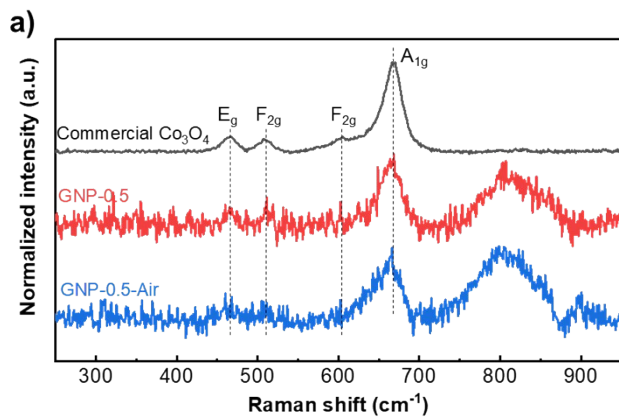


95

96 Figure S13 Specific COOH surface concentration and geometric current density at an overpotential of 450 mV of GNP-

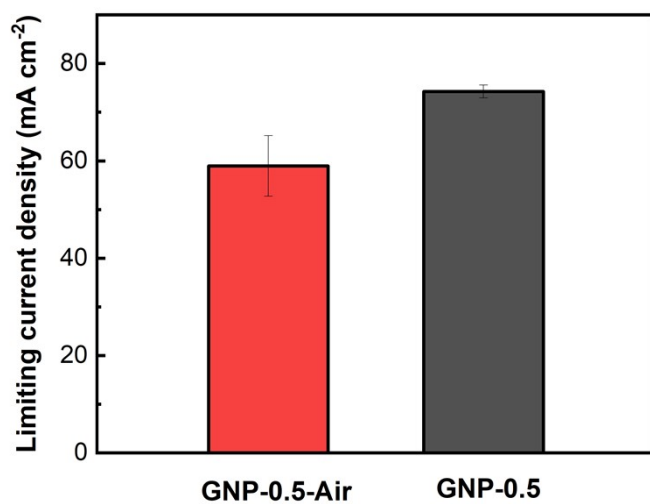
97 0.5-Air and GNP-0.5.

98



99

100 Figure S14 a) Raman spectroscopy including the peaks of Co_3O_4 , acquired on GNP-0.5, GNP-0.5-Air and on commercial
 101 Co_3O_4 . b) the Tafel slopes of GNP-0.5 and GNP-0.5-Air

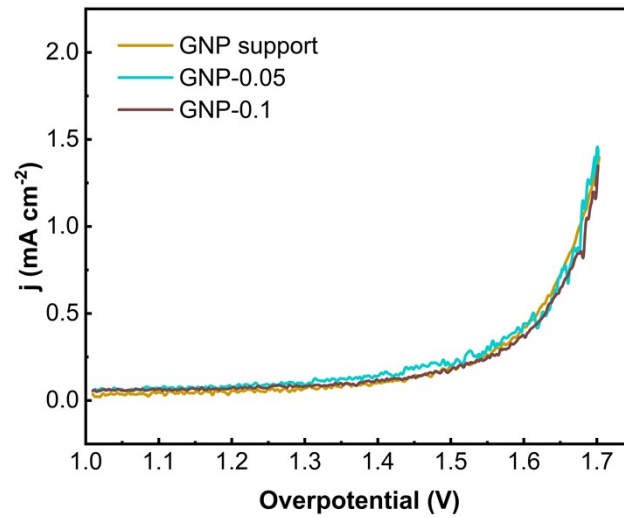


103

104 Figure S15 Summary of the limiting current density, calculated from LSV of GNP-0.5-Air and GNP-0.5, in Fe-free KOH

105 1M, scanned from 1.5 to 2.2 V vs RHE at a scan rate of 10 mV s⁻¹. The potential was corrected with 85% of iR-drop.

106



107

108 Figure S16 CVs of GNP, GNP-0.05 and GNP-0.1 loadings in Fe-free 1M KOH solution, scanned from 1.0–1.7 V vs RHE
109 at a scan rate of 10 mV s⁻¹. CV curves were iR-corrected (85% iR drop compensation) and averaged across the forward
110 and backward scans.

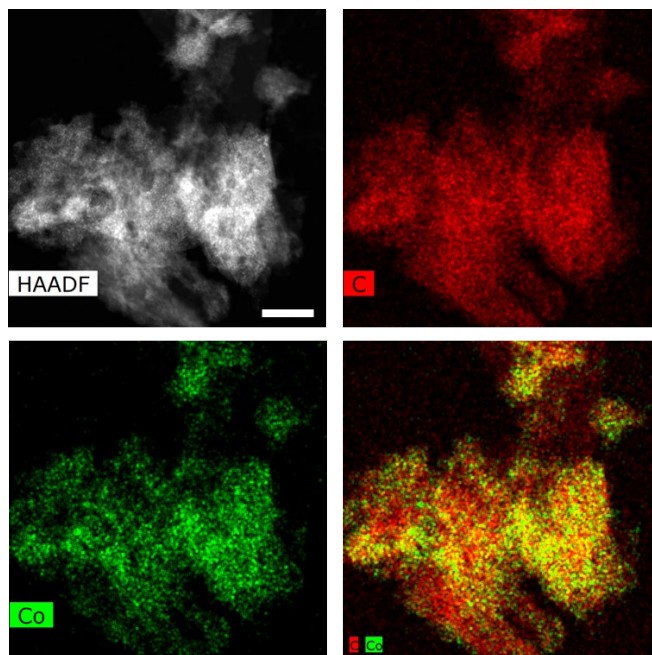
111

112 Table S7 Co contents in the synthesized catalysts with different Co loadings: GNP-0.5, GNP-4.8, GNP-9.1, GNP-17 and
113 GNP-29, averaged from 3 sets of measurements

Theoretical loading	Co concentration by ICP-OES
0.5	0.51 ± 0.01
4.8	4.67 ± 0.71
9.1	10.88 ± 0.21
17	17.72 ± 4.33
29	29.62 ± 6.81

114

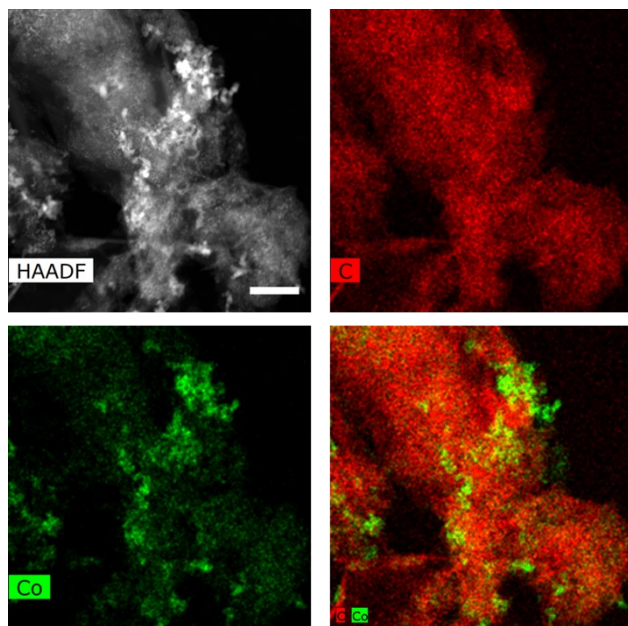
115



116

117 Figure S17 HAADF-STEM images and the corresponding elemental maps for C and Co of GNP-4.8. Scale bar: 100 nm.

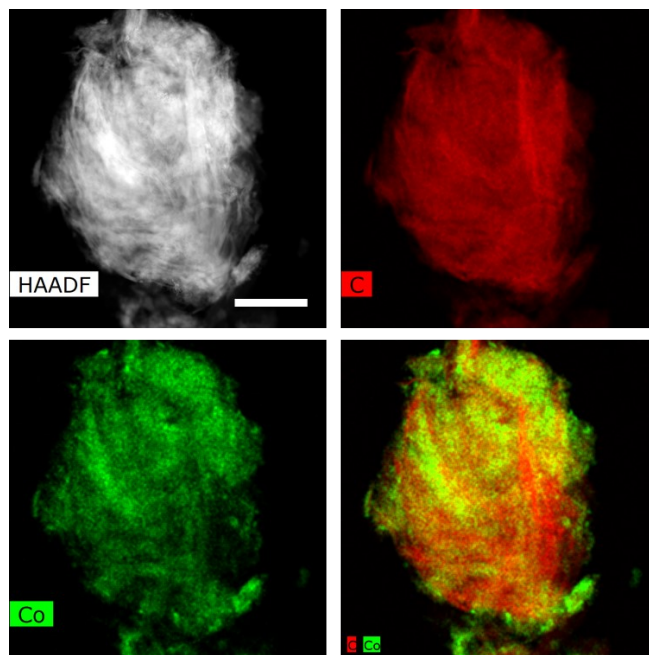
118



119

120 Figure S18 HAADF-STEM images and the corresponding elemental maps for C and Co of GNP-9.1. Scale bar: 100 nm.

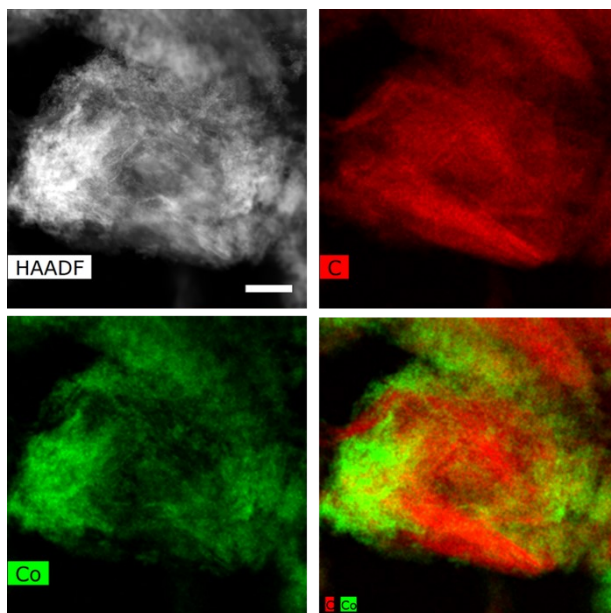
121



122

123 Figure S19 HAADF-STEM images and the corresponding elemental maps for C and Co of GNP-17. Scale bar: 1 μm .

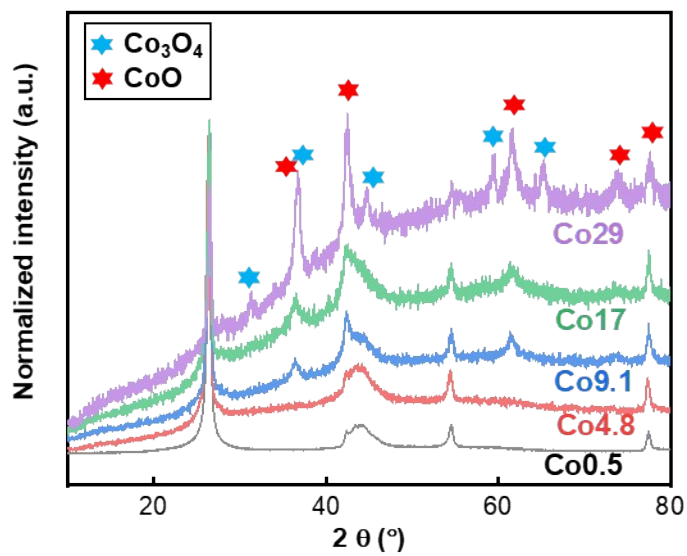
124



125

126 Figure S20 HAADF-STEM images and the corresponding elemental maps for C and Co of GNP-29. Scale bar: 200 nm.

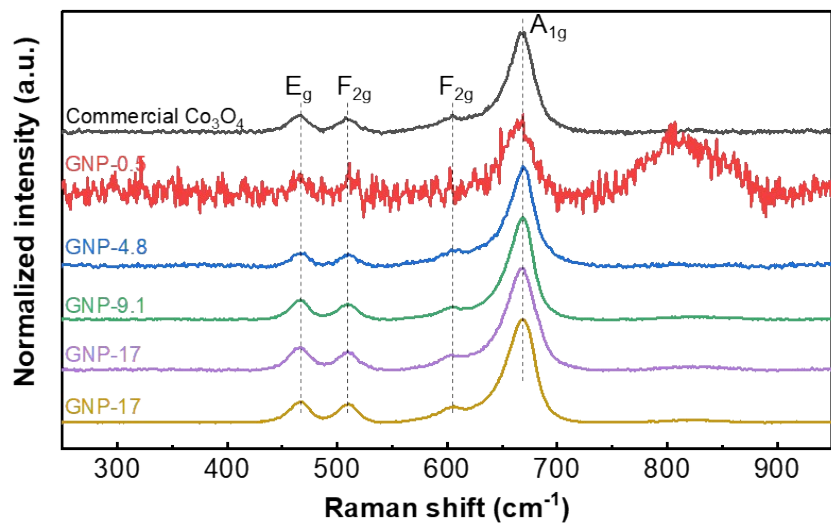
127



128

129 Figure S21 XRD patterns of the Co-based catalysts supported on GNP at different Co loadings and the reference bulk
130 oxide phases (CoO PDF 1541662, Co_3O_4 PDF 1548531)

131



132

133 Figure S22 Raman spectroscopy including the peaks of Co₃O₄, acquired on Co-catalyst supported on GNP at various
134 Co loadings and on commercial Co₃O₄.

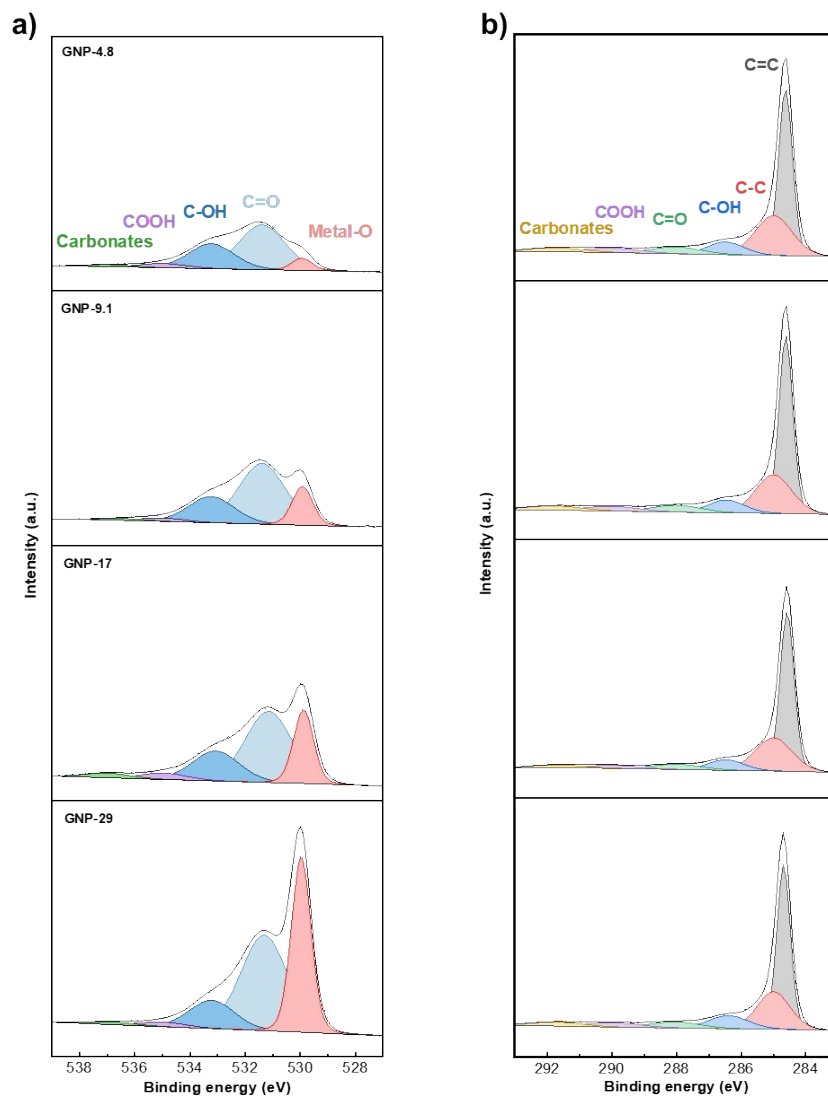
135

136 Table S8 Summary of I_d/I_g ratio of the Co-based catalysts supported on GNP at different Co loadings, determined with
137 Raman spectroscopy. The presented value was obtained from at least 10 different regions. The gain in I_d/I_g between
138 before and after Co-incorporation is calculated as the quotient between $[I_d/I_{g[\text{Co-doped}]} - I_d/I_{g[\text{fresh GNP}]}]$ and $[I_d/I_{g[\text{fresh GNP}]}]$.

Co loading	I_d/I_g	Gain in I_d/I_g (%)
0	0.114 ± 0.023	
0.5	0.148 ± 0.056	29.410
4.8	0.154 ± 0.085	34.586
9.1	0.141 ± 0.034	23.434
17	0.140 ± 0.023	22.065
29	0.154 ± 0.051	34.250

139

140



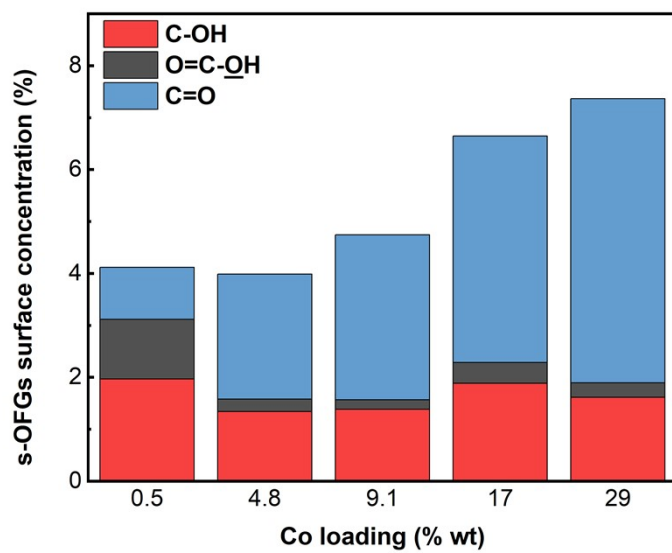
141

142 Figure S23 XPS spectra of different Co-catalyst supported on GNP, at various Co loadings. a) XPS O 1s spectra and b)

143 XPS C 1s spectra and the corresponding deconvoluted peaks.

144

145



146

147 Figure S24 Surface concentration of COH, COOH and C=O, measured on Co-based catalysts supported on GNP at
148 different Co loadings.

149

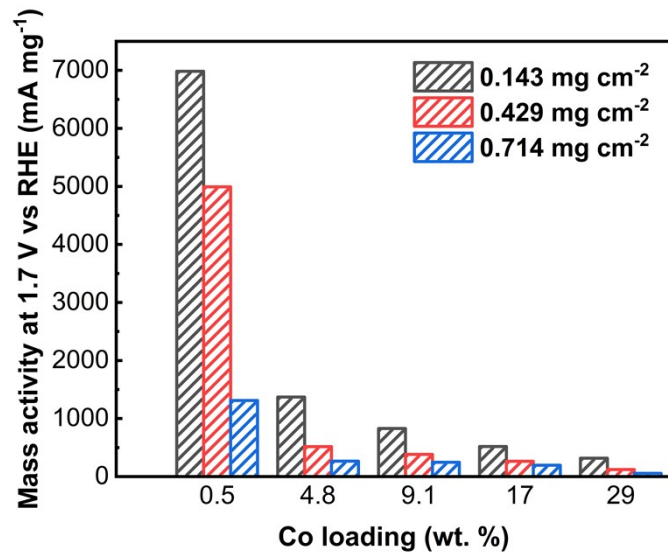
150

151 Table S9 Summary of the surface concentration of COH, COOH and C=O, measured on Co-based catalysts supported
152 on GNP at different Co loadings.

Co loading (%)	C-OH	O=C-OH	C=O
0.5	1.96	1.15	1.00
4.8	1.34	0.24	2.41
9.1	1.39	0.18	3.18
17	1.89	0.40	4.36
29	1.62	0.28	5.47

153

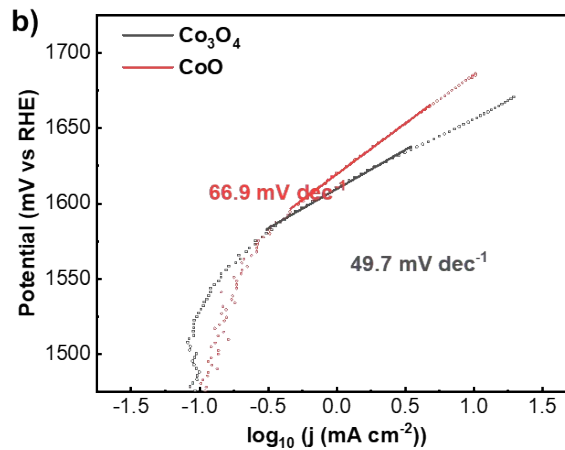
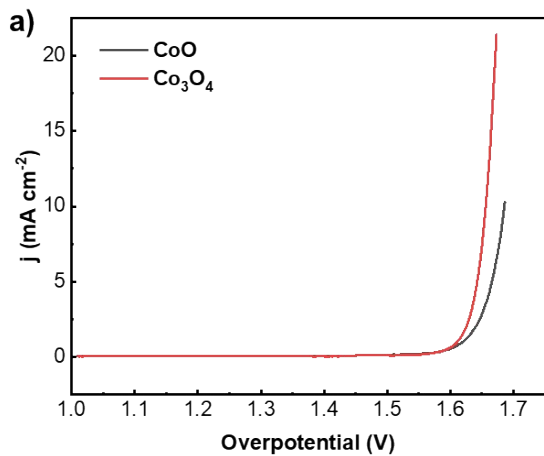
154



155

156 Figure S25 Summary of the mass activities at 1.7 V vs RHE of GNP-0.5, GNP-4.8, GNP-9.1, GNP-17 and GNP-29 in Fe-
 157 free 1M KOH solution, at various surface loadings.

158



159

160 Figure S26 OER activity of commercial CoO and Co₃O₄. a) CV in Fe-free KOH 1M, scanned from 1.0 to 1.7 V vs RHE at
 161 a scan rate of 10 mV s⁻¹. The curves were corrected with 85% of iR-drop, and averaged from onward and backward
 162 scans. b) The corresponding Tafel slopes.

163

164 Table S10 Summary of the surface concentration of COH, COOH and C=O, measured on Co-based catalysts supported
165 on GNP at different Co loadings, normalized by the Co mass loading of the samples.

Co loading (%)	Co-normalized C-OH (%)	Co-normalized O=C-OH (%)	Co-normalized C=O (%)	Co-normalized I_d/I_g
0.5	3.929	2.305	1.998	0.296
4.8	0.279	0.050	0.502	0.032
9.1	0.152	0.020	0.349	0.016
17	0.111	0.023	0.257	0.008
29	0.056	0.010	0.189	0.005

166

167

168 **REFERENCES**

- 169 [1] P. Kumar, K. Kannimuthu, A. S. Zeraati, S. Roy, X. Wang, X. Wang, S. Samanta, K. A. Miller, M. Molina,
170 D. Trivedi, J. Abed, M. A. Campos Mata, H. Al-Mahayni, J. Baltrusaitis, G. Shimizu, Y. A. Wu, A.
171 Seifitokaldani, E. H. Sargent, P. M. Ajayan, J. Hu, M. G. Kibria, *J. Am. Chem. Soc.* **2023**, *145*, 8052.
- 172 [2] R. Lu, D. K. Sam, W. Wang, S. Gong, J. Liu, A. Durairaj, M. Li, X. Lv, *J. Colloid Interface Sci.* **2022**, *613*,
173 126.
- 174 [3] L. Yang, H. Liu, H. Shen, Y. Huang, S. Wang, L. Zheng, D. Cao, *Adv. Funct. Mater.* **2020**, *30*, 1.
- 175 [4] A. W. Jensen, G. W. Sievers, K. D. Jensen, J. Quinson, J. A. Arminio-Ravelo, V. Brüser, M. Arenz, M.
176 Escudero-Escribano, *J. Mater. Chem. A* **2020**, *8*, 1066.
- 177 [5] P. Jash, P. Srivastava, A. Paul, *Chem. Commun.* **2019**, *55*, 2230.
- 178 [6] C. Cai, S. Han, X. Zhang, J. Yu, X. Xiang, J. Yang, L. Qiao, X. Zu, Y. Chen, S. Li, *RSC Adv.* **2022**, *12*, 6205.
- 179 [7] J. Huang, J. Chen, T. Yao, J. He, S. Jiang, Z. Sun, Q. Liu, W. Cheng, F. Hu, Y. Jiang, Z. Pan, S. Wei, *Angew.*
180 *Chemie - Int. Ed.* **2015**, *54*, 8722.
- 181 [8] M. Kim, B. Lee, H. Ju, S. W. Lee, J. Kim, *Adv. Mater.* **2019**, *31*, 1.
- 182 [9] A. Bähr, H. Petersen, H. Tüysüz, *ChemCatChem* **2021**, *13*, 3824.
- 183 [10] Y. R. Hong, S. Mhin, K. M. Kim, W. S. Han, H. Choi, G. Ali, K. Y. Chung, H. J. Lee, S. I. Moon, S. Dutta, S.
184 Sun, Y. G. Jung, T. Song, H. S. Han, *J. Mater. Chem. A* **2019**, *7*, 3592.

185